Spring 5-30-2024

Anion Binding and Sensing Using Cs124-Sensitized Luminescent Terbium Complexes

Alessandro Rizzi

Minhee Lee
Seattle Pacific University

Wade Grabow

Olivia Brooks

Helena Nguyen

See next page for additional authors

Anion Binding and Sensing Using Cs124-Sensitized Luminescent Terbium Complexes

By

Alessandro Rizzi

Faculty Mentor:

Dr. Minhee Lee, Department of Chemistry and Biochemistry, Seattle Pacific University

Honors Program Director:

Dr. Joshua Tom

A project submitted in partial fulfillment of the requirements

for the Bachelor of Arts degree in Honors Liberal Arts

Seattle Pacific University

2024

Presented at the SPU Honors Research Symposium

5/18/2024

Abstract: Two terbium complexes with varying degrees of intramolecular coordination, Tb:DO2A-Cs124 and Tb:DOTA-Cs124, were prepared. Their capacity to detect biologically and environmentally relevant anions through their luminescence changes was investigated. Tb:DOTA-Cs124 demonstrated exceptional selectivity as a sensor for nitrite, while Tb:DO2A-Cs124 detects nitrite, phosphates, and a range of carboxylate-containing anions.

ChemComm

COMMUNICATION

Anion Binding and Sensing Using Cs124-Sensitized Luminescent Terbium Complexes

Received 00th January 20xx,
Accepted 00th January 20xx

DOI: 10.1039/x0xx00000x

Alessandro Rizzi [a], Wade Grabow[a], Olivia Brooks [a], Helena Nguyen [a], Neal Yakelis[b], Clarisse VanderFeltz[c], and Minhee Lee *[a]

Two terbium complexes with varying degrees of intramolecular coordination, Tb:DO2A-Cs124 and Tb:DOTA-Cs124, were prepared. Their capacity to detect biologically and environmentally relevant anions through their luminescence changes was investigated. Tb:DOTA-Cs124 demonstrated exceptional selectivity as a sensor for nitrite, while Tb:DO2A-Cs124 detects nitrite, phosphates, and a range of carboxylate-containing anions.

Over recent decades, significant research efforts have been put towards developing lanthanide complexes as luminescent sensors for anions, particularly in the realms of biochemical and environmental applications.[1] These lanthanide complexes, usually containing Tb^{3+} or Eu^{3+}, possess unique photophysical properties that are desirable for optical sensors. These includes large Stokes shift, sharp line-like emission bands in a useful wavelength domain (500-700 nm), and long luminescence lifetime (in the order of a few milliseconds), allowing time-gated background-free measurement and high detection sensitivity for target analytes.[2]

A few different anion-sensing strategies for luminescent lanthanide complexes have been employed, including promotion of new interactions between an anion and a lanthanide metal to induce a luminescent property change. For instance, Parker et al. demonstrated the efficacy of Eu^{3+} complexes containing an azaxanthone photo-antenna and a DO3A-based heptadentate ligand in detecting bicarbonate, citrate, and lactate.[3,4] Additionally, Pierre et al. synthesized a series of tripodal Eu^{3+} complexes with a hexadentate ligand for the detection of HPO_4^{2-}.[5] In both studies, detection of the anion was achieved through changes in the coordination environment of the Eu^{3+} where anions can competitively bind to displace either intramolecularly bound carboxylates or intermolecularly bound water molecules.

Herein, we present how octa- or hexa-dentated Tb complexes containing carbostyril 124 (Cs124) as an organic antenna can be utilized as sensors for anions, after screening their luminescence properties in the presence of various anions including halides, oxoanions ($A_xO_z^{-y}$, A = C, N, P, S), nucleotides, and metabolic carboxylates. Cs124 is efficient in sensitizing Tb^{3+} luminescence,[6] chemically inert, resistant to photobleaching, and can be readily synthesized in one step. Consequently, Cs124 has emerged as a compelling option as an organic antenna for terbium complexes, which are designed as probes for biological sensing or imaging. These terbium complexes typically incorporate a highly coordinative ligand (e.g., 1,4,7,10-tetraazacyclododecane-1,4,7,10-tetraacetic acid or DOTA), which binds tightly to Tb^{3+} to mitigate its cytotoxic effects. Nevertheless, the luminescence characteristics of these complexes in the presence of various biologically or environmentally significant anions remain unexplored. We embarked on addressing this inquiry to enhance the accurate interpretation of data acquired from complex media, such as live cells and environmental samples. Additionally, we examined how substituting the octadentate ligand with a hexadentate ligand (e,g., 1,4,7,10-tetraazacyclododecane-1,7-diacetic acid or DO2A) could impact the complex's interaction with anions and ultimately its luminescence. DO2A is known to form a highly stable complex with Tb^{3+} in aqueous solutions ($\log K = 12.93 \pm 0.01$), while still allowing Tb^{3+} sites for water molecules to chelate. As the O-H oscillators of these nearby water molecules non-radiatively deactivate terbium's excited state, we hypothesized that certain anions enhance the luminescence of Tb^{3+} by displacing the water molecules.

Two terbium complexes, $[Tb:DOTA\text{-}Cs124]^0$ and $[Tb:DO2A\text{-}Cs124]^{2+}$, each possessing distinct net charges, were prepared (**Scheme 1**, see supporting info for detailed synthetic procedures). First, we synthesized N-Boc-protected cyclen derivatives containing varying number of tert-butyl-protected acetic acid moieties (1 and 2, respectively) by following previously described methods.[7] Cs124 was incorporated to the ligands by N-alkylation with 3, followed by global

[a] *Department of Chemistry and Biochemistry, Seattle Pacific University 3307 3rd Ave W, Seattle, WA 98119 USA*
[b] *Department of Chemistry, Pacific Lutheran University, Tacoma, WA 98447 USA*
[c] *Department of Biology, Northwest University, Kirkland, WA 98033 USA*

*email: leem23@spu.edu

Electronic Supplementary Information (ESI) available: [details of any supplementary information available should be included here]. See DOI: 10.1039/x0xx00000x

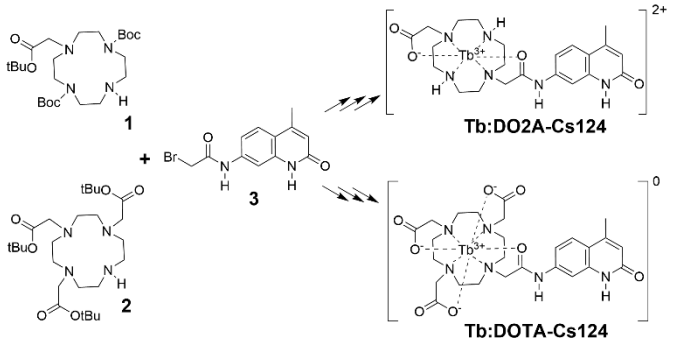

Scheme 1. Synthesis of Tb:DO2A-Cs124 and Tb:DOTA-Cs124. Reagents and conditions: See supplemental information.

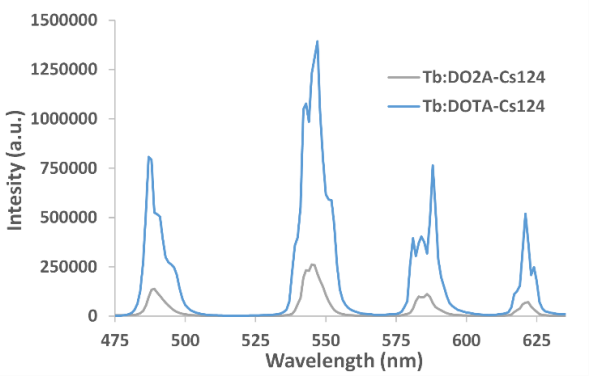

Figure 1. Luminescent spectra of Tb:DO2A-Cs124 and Tb:DOTA-Cs124. Experimental condition: [Tb:DO2A-Cs124] or [Tb:DO2A-Cs124] = 10 μM in d.H_2O, pH 7, λ_{ex} = 340 nm.

deFSprotection, purification via preparative RP-HPLC, and complexation with a stoichiometric amount of Tb^{3+}. Subsequently, we tested the luminescence properties of Tb:DOTA-Cs124 and Tb:DO2A-Cs124. Bright green emission, that is characteristic of Tb^{3+} luminescence, was observed from Tb:DOTA-Cs124 while emission from Tb:DO2A-Cs124 (**Figure 1**) was significantly weaker due to increased number of water molecules directly chelated to Tb^{3+} (q). These inner sphere water molecules are known to quench Tb^{3+} luminescence via nonradiative vibrational energy transfer.[1] Indeed, *q* values were determined to be 2.36 and 0.85 for Tb:DO2A-Cs124 and Tb:DOTA-Cs124, respectively, by comparing their luminescence lifetimes in H_2O versus D_2O from time-resolved emission experiments (**Table 1**) using the equation (1).[8] Where for terbium, A is 5 ms and B is 0.06 ms^{-1}. Given that Tb^{3+} has 9 available coordination sites, these q values are in good concordance with the expected values, i.e., 3 for DO2A and 1 for DOTA.

$$q = A * \left(\frac{1}{\tau_{H2O}} - \frac{1}{\tau_{D2O}} - B\right) \text{(1)}$$

Next, we examined whether specific anions could replace these inner sphere water molecules and affect luminescence of these complexes. Tb:DOTA-Cs124 exhibited strikingly unperturbed emission profile in the presence of various anions except for NO_2^- (**Figure 2a**). This suggests that interactions of anions to Tb^{3+} center is not strong in the octadentate neutral

Added Anion	τ_{H2O} (ms)	τ_{D2O} (ms)	*q*
Tb:DO2A-Cs124	0.98	2.02	2.36
Tb:DOTA-Cs124	1.59	2.50	0.85

Table 1. Luminescent lifetimes of Tb:DO2A-Cs124 and Tb:DOTA-Cs124 in H_2O and D_2O and nu (*q*) of Tb:DO2A-Cs124 and Tb:DOTA-Cs124. Experimental condition: [Tb:DO2A-Cs124] or [Tb:DO2A-Cs124] = 10 μM in d.H_2O, pH 7, λ_{ex} = 340 nm.

DOTA system as a result of decreased accessibility of anions to the metal center and weaker Columbic attraction.

In the presence of 100 equivalents of NO_2^-, Tb:DOTA's luminescence became quenched by 70%. Energy transfer from $^5D_4$ excited state of Tb^{3+} (20,500 cm^{-1}) to triplet energy state of NO_2^- (19,084 cm^{-1}) is known to be efficient.[9], although it has limited precedent. Since the hydration number in the Tb:DOTA-Cs124 did not change upon addition of NO_2^- (**Table S2**), we postulate that the quenching is likely the result of energy transfer between freely diffusing species and their bimolecular collision. We further investigated the nature of the quenching by titration experiments with increasing concentrations of NO_2^- (**Figure 2b**). The resulting data was utilized in the Stern–Volmer (S–V) equation (2) to determine the quenching constant (K_{SV}) as 2.18 x 10^3 M^{-1}.

$$\frac{I_0}{I} - 1 = K_{SV}[C] \text{ (2)}$$

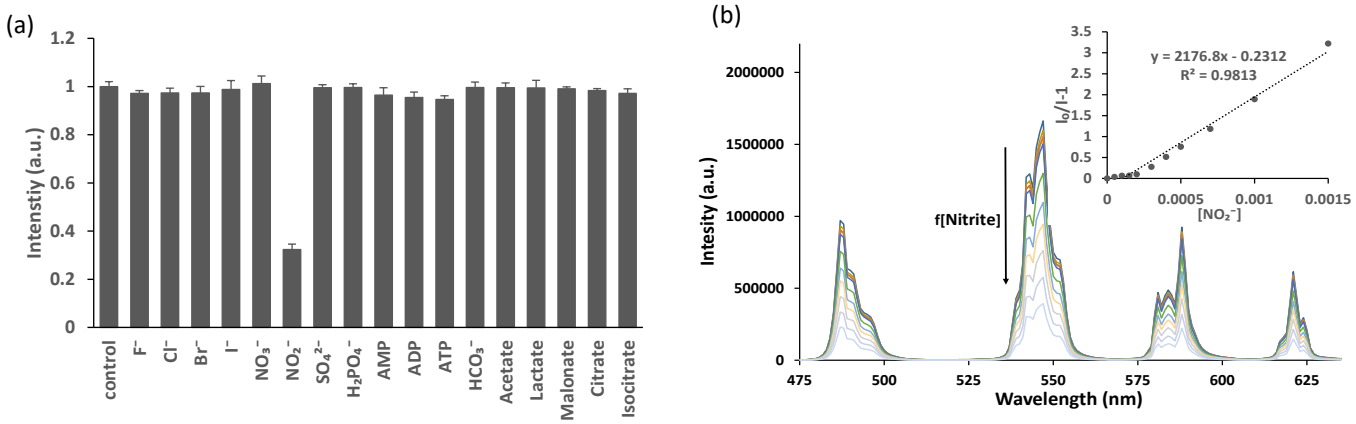

Figure 2. a) Emission of Tb:DOTA-Cs124 in the presence of various anions. Experimental condition: [Tb:DOTA-Cs124] = 10 μM in H_2O, pH 7, [anion] = 1 mM, λ_{ex} = 340 nm. Intensity is the normalized sum of emission intensities from 530 – 560 nm based on the control in the absence of anions. b) Decrease in luminescence intensity of Tb:DOTA-Cs124 by addition of NO_2^-. Experimental condition: [Tb:DOTA-Cs124] = 10 μM in H_2O, pH 7, [anion] = 0 – 1.5 mM, λ_{ex} = 340 nm. Inset: S–V plots of Tb:DOTA-Cs124 shown as I_0/I as a function of [NO_2^-]. I_0 and I are luminescent intensity of Tb:DOTA-Cs124 in the absence and presence of NO_2^-, respectively.

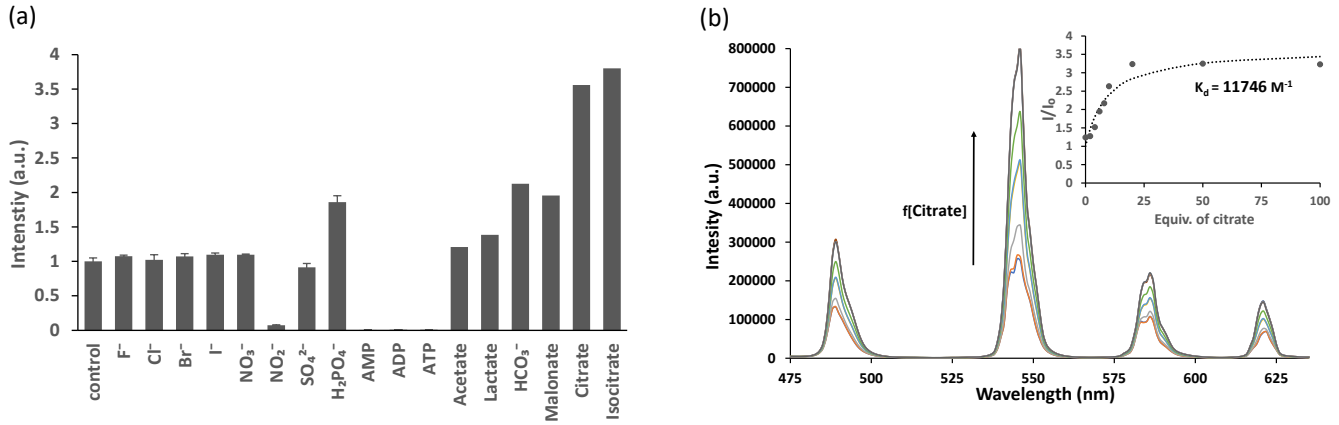

Figure 3. a) Emission of Tb:DO2A-Cs124 in the presence of various anions. Experimental condition: [Tb:DO2A-Cs124] = 10 μM in H_2O, pH 7, [anion] = 1 mM, λ_{ex} = 340 nm. Intensity is the normalized sum of emission intensities from 530 – 560 nm based on the control in the absence of anions. b) Increase in luminescence intensity of Tb:DO2A-Cs124 by addition of citrate. Experimental condition: [Tb:DOTA-Cs124] = 10 μM in H_2O, pH 7, [citrate] = 0 – 1 mM, λ_{ex} = 340 nm. Inset: Titration curve of Tb:DO2A-Cs124 shown as I/I_0 as a function of equivalents of citrate added.

The emission profile of Tb:DO2A-Cs124 exhibited more pronounced dynamic changes upon addition of anions compared to its DOTA analogue (**Figure 3a**), presumably due to anions' enhanced accessibility and stronger Columbic attraction to the Tb^{3+} center. All halides, NO_3^-, and SO_4^{2-} again had negligible effects on Tb:DO2A-s124's emission while NO_2^- showed more profound quenching effect. $H_2PO_4^-$ increased luminescence by 2-fold, which can be explained by a decrease in hydration state as $H_2PO_4^-$ binds to Tb^{3+} and displace water molecules (**Table S1**). However, phosphate containing nucleotides (AMP, ADP, and ATP) substantially diminished Tb:DO2A-124's luminescence, presumably between excited singlet state of the Cs124 antenna and electron-rich adenine,[10] facilitated by phosphate's binding to the Tb^{3+}. Carboxylate-containing anions (bicarbonate, acetate, lactate, malonate, and citrate) enhanced luminescence by varying degrees, generally more enhancement by anions with higher number of carboxylate groups. The largest emission increase (>3.5-fold increase) was observed by citrate and isocitrate containing three carboxylate groups. We expect that citrate displaces three inner sphere water molecules (**Figure 4**), and this suggested model is consistent with hydration state change from 2.6 to 0.3 (**Table S1**) in the presence of citrate. We carried out titration experiment for Tb:DO2A-Cs124 with increasing concentration of citrate, and the resulting data was fitted to a 1:1 host-guest binding mode to determine K_a value as 11746 M^{-1}.[11]

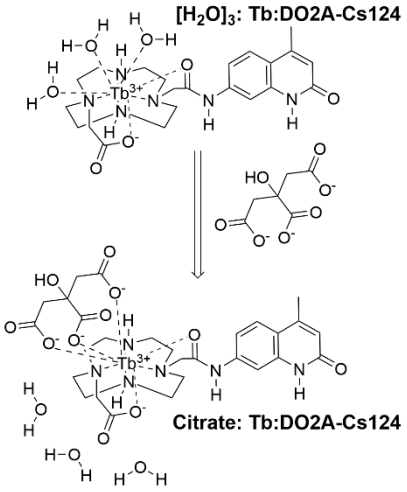

Figure 4. Proposed model for the observed luminescence increase of Tb:DO2A-Cs124 by binding of citrate to Tb^{3+} displacing water molecules.

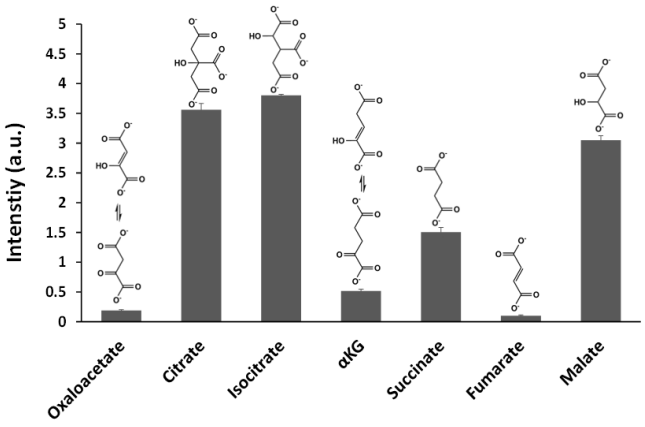

Figure 5. Emission of Tb:DO2A-Cs124 in the presence of citric acid cycle intermediates. Experimental condition: [Tb:DO2A-Cs124] = 10 μM in H_2O, pH 7, [anion] = 1 mM, λ_{ex} = 340 nm. Intensity is the normalized sum of emission intensities from 530 – 560 nm based on the control in the absence of anions.

Intrigued by Tb:DO2A-Cs124's ability to sense various carboxylate containing anions, we examined how its luminescence responds to an extended set of metabolites involved in the citric acid cycle (**Figure 5**). All these metabolites contain one or more carboxylate groups, enabling them to bind to Tb^{3+} and possibly enhance its emission like citrate does. Indeed, succinate and malate increased Tb:DO2A-Cs124's emission by 1.5- and 3-fold, respectively. However, to our surprise, three other metabolites (oxaloacetate, a-ketoglutarate, and fumarate) unexpectedly resulted in luminescence quenching. Drawing from shared structural characteristics observed among these three metabolites, we postulate that the quenching phenomenon arises from energy transfer from the excited state of terbium to the triplet energy state of an extended π-conjugated system present in α,β-

unsaturated carboxylates, which oxaloacetate and fumarate can generate through keto-enol tautomerization.[12]

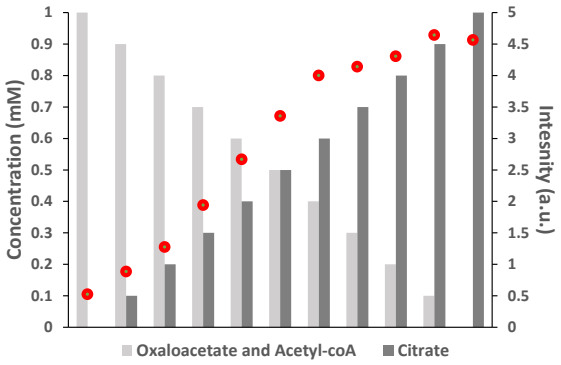

Figure 6. Emission of Tb:DO2A-Cs124 (shown as red dots) in the presence of varying concentrations of oxaloacetate, acetyl CoA, and citrate (shown as bar graphs). Experimental condition: [Tb:DO2A-Cs124] = 10 μM in H_2O, pH 7, λ_{ex} = 340 nm, λ_{em} =530 – 560 nm.

Lastly, as proof of principle, we explored the potential application of Tb:DO2A-Cs124 in monitoring the first reaction of the citric acid cycle, i.e., conversion of oxaloacetate. This reaction is anticipated to result in a substantial increase in emission, based on our observation that not only oxaloacetate but acetyl-CoA were found to quench the luminescence of Tb:DO2A-Cs124 (**Figure S5**) whereas citrate strongly enhances the emission. The overall metabolic flux of the citric acid cycle is governed by the activity of citrate synthase, the enzyme responsible for catalyzing this reaction. Consequently, dysregulated activity of citrate synthase is implicated in numerous human diseases, including cancers and various metabolic disorders, urging the need for the development of more tools capable of monitoring this enzyme's activity. Solutions were prepared containing increasing concentrations of citrate, and decreasing concentrations of acetyl-CoA and oxaloacetate to simulate the progression of the citrate synthase-catalyzed reaction (**Figure 6**). The emission spectra obtained from these solutions showed a continuous increase in accordance with the simulated progression of the reaction. Overall, there was a nine-fold increase observed upon the complete conversion of acetyl-CoA and oxaloacetate to citrate, suggesting the potential use of Tb:DO2A-Cs124 as a luminescent enzyme activity probe for citrate synthase. Similarly, Tb:DO2A-Cs124 can also be utilized to monitor other crucial reactions within the citric acid cycle by leveraging the contrasting effects of two adjacent intermediates on the emission.

In summary, we have demonstrated the development of two terbium complexes with differential metal chelation states, Tb:DO2A-Cs124 and Tb:DOTA-Cs124, for the purpose of sensing anions. Utilizing Tb:DOTA-Cs124, we achieved highly selective detection of NO_2^- amidst a diverse range of anions, suggesting a promising application for this complex in detecting NO_2^- within complex cellular or environmental media. Meanwhile, Tb:DO2A-Cs124 complex is responsive to specific groups of anions such as NO_2^-, $H_2PO_4^-$, adenosine phosphates, and various carboxylate containing anions. Citrate, a crucial tricarboxylate metabolite in the citric acid cycle, notably induced a 3.5-fold enhancement of emission by binding to Tb^{3+} and displacing three inner-sphere water molecules. Our findings highlight the potential utility of Tb:DO2A-Cs124 as an enzyme activity probe for citrate synthase and other enzymes involved in the citric acid cycle, as well as for evaluating inhibitors and competitive substrates for these enzymes, *in vitro*. For both complexes, the long radiative lifetimes of Tb^{3+} enables highly sensitive, background-free measurement. Moreover, efficient sensitization of Eu^{3+} or Dy^{3+} can also be achieved by simple and systematic derivatization of Cs124 to program the emission output in the red or near IR regions, which is previously reported.[13]

Conflicts of interest

There are no conflicts to declare.

Notes and references

The authors acknowledge the use of facilities and instrumentation supported by NSF through the UW Molecular Engineering Materials Center (MEM-C), a Materials Research Science and Engineering Center (DMR- 2308979)

1 (a) S.E. Bodman, and J.B Stephen. *Chemical Science*, 2021, **12**, 2716-2734.(b) M. C. Heffern, L. M. Matosziuk, and T. J. Meade. *Chemical reviews*, 2014, **114**, 4496-4539. (c) V. C. Pierre, and R. K. Wilharm. *Frontiers in Chemistry*, 2022, **10**, 821020. (d) M. L. Aulsebrook, B. Graham, M. R. Grace, and K. L. Tuck. *Coordination Chemistry Reviews*, 2018, **375**, 191-220. (e) U. Cho, and J. K. Chen. *Cell chemical biology*, 2020, **27**, 921-936.
2 (a) D. Parker, R. S. Dickins, H. Puschmann, C. Crossland, and J. A. Howard. *Chemical Reviews*, 2012, **102**, 1977-2010. (b) S. Faulkner, S. JA Pope, and B. P. Burton-Pye. *Applied Spectroscopy Reviews*, 2005, **40,** 1-31. (c) S. V. Eliseeva, and G. B. Jean-Claude. *Chemical Society Reviews*, 2010, **39**, 189-227.
3 R. Pal, D. Parker, and L. C. Costello. *Organic & biomolecular chemistry*, 2009, **7**, 1525-1528.
4 D. G. Smith, R. Pal, and D. Parker. *Chemistry–A European Journal*, 2012, **18**, 11604-11613.
5 M.V.R. Raju, S. M. Harris, and V. C. Pierre. C*hemical Society Reviews*, 2020, **49**, 1090-1108.
6 (a) S. Mizukami, K. Tonai, M. Kaneko, and K. Kikuchi. *Journal of the American Chemical Society,* 2008, **5,** 14376-14377. (b) M. Varga, Z. Kapui, S. Bátori, L.T. Nagy, L. Vasvári-Debreczy, E. Mikus, K. Urbán-Szabó, and P. Arányi. *European journal of medicinal chemistry*, 2003, **38**, 421-425.
7 (a)L. Min, and P. R. Selvin. *Journal of the American Chemical Society*, 1995, **117,** 8132-8138. (b)D. Parker, and W.J.A. Gareth. *Journal of the Chemical Society, Perkin Transactions*, 1996, **2**, 1581-1586.
8 *J. Chem. Soc., Perkin Trans.* ***2***, 1999, 493-504
9 (a) A. Treinin, and E. Hayon. *Journal of the American Chemical Society,* 1976, **98**, 3884-3891. (b) M. H. Zongsu Han, M. Wang, Y. Li, T. Zhou, W. Shi, and P. Cheng. *Inorganic Chemistry Frontiers*, 2020, 7, 3379-3385.
10 E. A. Weitz, J.Y. Chang, A.H. Rosenfield, E. A. Morrow, and V. C. Pierre. *Chemical Science*, 2013, **4**, 4052-4060.
11 http://supramolecular.org, accessed March 19, 2014.
12 Covey, W. D., and D. L. Leussing. *Journal of the American Chemical Society*, 1974, **96**, 3860-3866.
13 M.S. Tremblay, H. Marlin, and S. Dalibor. *Journal of the American Chemical Society*, 2007, **129**, 7570-7577.

Supporting Information

Anion Binding and Sensing Using Cs124-Sensitized Luminescent Terbium Complexes

Alessandro Rizzi,[a] Wade Grabow, [a] Olivia Brooks,[a] Helena Nguyen,[a] Neal Yakelis,[b] Clarisse VanderFeltz,[c] and Minhee Lee [a,*]

[a]*Department of Chemistry and Biochemistry, Seattle Pacific University 3307 3rd Ave W, Seattle, WA 98119 USA*

leem23@spu.edu

[b]*Department of Chemistry, Pacific Lutheran University, Tacoma, WA 98447 USA*

[c]*Department of Biology, Northwest University, Kirkland, WA 98033 USA*

Part I: Synthetic Methods

Materials and general methods

Unless otherwise noted, all chemicals were purchased from Sigma-Aldrich or Fisher Scientific and used without further purification. Flash chromatography was performed on SILICYCLE silica gel (230–400 mesh). Nuclear Magnetic Resonance spectra were recorded at 300 K (unless otherwise noted) on Bruker AV300 or NEO500 Fourier transform NMR spectrometers. Proton chemical shifts are expressed in parts per million (ppm, δ scale) and are referenced to residual protium in the NMR solvent ($CDCl_3$, δ 7.26; CD_3OD, δ 3.31; DMSO, δ 2.50). Data for ^1H NMR are reported as follows: chemical shift, integration, multiplicity (s = singlet, d = doublet, t = triplet, m = multiplet, bs = broad singlet), and coupling constant in hertz (Hz). Carbon chemical shifts are expressed in parts per million (ppm, δ scale) and are referenced to the carbon resonance of the NMR solvent (DMSO, δ 39.52). Low-resolution mass spectra were obtained using a Bruker Esquire LC Ion Trap (ionization mode: $APCI^+$) integrated with Agilent 1100 liquid chromatograph system. Preparative HPLC was performed with a Rainin Dynamax SD200 controller on a Waters Delta-Pak C1 column (#11804); fractions were detected with a Rainin Dynamax UV-C detector and collected with a Varian model FC-701 Sample Manager. Data was analyzed using Varian Star LC Workstation (ver. 6.30). Isocratic elution or linear gradients of solvents A and B were used (A = HPLC grade acetonitrile or methanol containing 10% (v/v) de-ionized water; B = deionized water containing 0.1% (v/v) trifluoroacetic acid (ReagentPlus grade, 99%). High-resolution mass spectra were obtained on a Thermo Scientific (Waltham, MA) Q-Exactive HF-X mass spectrometer with a heated electrospray (HESI) source, coupled to a Thermo Vanquish Horizon UHPLC system. Data were obtained in the positive ionization mode at 240k resolution (at 200 m/z). Aliquots of the purified material were analyzed as loop injections using an isocratic gradient of 70/30 water:methanol, with 0.1% formic acid added to the buffer.

- Synthesis of 3

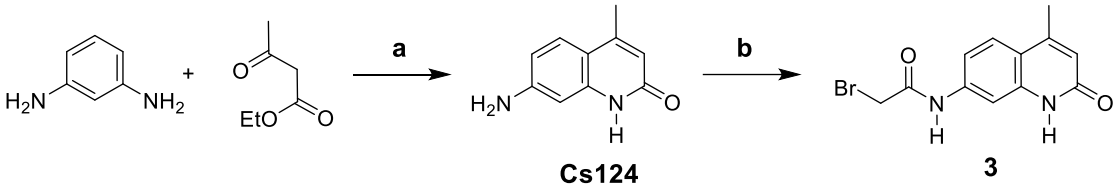

Scheme S1. Conditions: (a) Ethyl acetyl acetate, 150 °C, 20 h, 21%; (b) bromoacetyl bromide, $NaHCO_3$, MeCN, rt, 24 h, 66%.

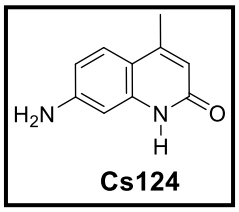

A reaction mixture containing phenylenediamine (1.0 g, 5.3 mmol) and ethyl acetyl acetate (6.3 mL, 5.3 mmol) was heated under argon at 150 °C. After 20 hours, the solution was cooled from which the crude product was recrystallized from MeOH, yielding an off-white solid. The solid was washed with hexanes and Et_2O, and then dried under high vacuum to afford Cs124 as a white solid (21%). ^{1}H NMR (DMSO-d_6, 500 MHz): δ 11.16 (1H, s), δ 7.33 (1H, d, *J* = 8.6 Hz), 6.45 (1H, d, *J* = 8.5 Hz), 6.37 (1H, s), 5.95 (1H, s), 5.73 (2H, s), 2.27 (3H, s). ^{13}C NMR (DMSO-d_6, 500 MHz): 162.41, 151.06, 147.94, 140.77, 125.56, 114.66, 110.43, 110.40, 96.80, 18.44. LRMS (APCI$^+$): Calculated for $C_{10}H_{10}N_2O$, expected *m/z* 174.1, measured *m/z* 175.2 [MH^+].

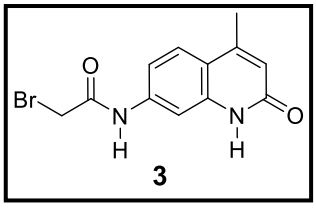

To compound Cs124 (1.2 g, 6.8 mmol) and $NaHCO_3$ (2.9 g, 34 mmol) in DMF (15 mL), bromoacetobromide (2.8 g, 14 mmol) in DMF (10 mL) was added dropwise at 0 °C and reacted at room temperature. After 24 h, the resulting precipitate was filtered and washed by d.H_2O to yield 3 as an ivory solid (66%). ^{1}H NMR (DMSO-d_6, 500 MHz) : δ 11.64 (1H, s), δ 10.66 (1H, s), δ 7.76 (1H, s), δ 7.66 (1H, d, *J* = 8.5 Hz), 7.33 (1H, d, *J* = 9 Hz), 6.29 (1H, s), 4.08 (2H, s), 2.38 (3H, s). ^{13}C NMR (DMSO-d_6, 500 MHz): 165.2, 161.9, 147.7, 140.3, 139.3, 125.5, 119.2, 116.0, 113.5, 104.7, 61.95, 18.4. LRMS (APCI$^+$): Calculated for $C_{12}H_{11}BrN_2O_2$, expected *m/z* 294.0, measured *m/z* 295.2 [MH^+].

- Synthesis of Tb:DO2A-Cs124

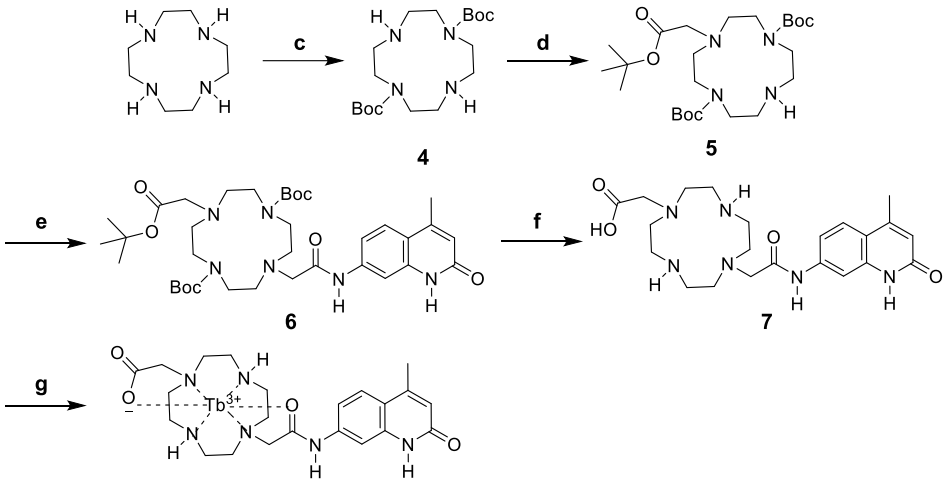

Scheme S2. Conditions: (c) Boc-OSu, $CHCl_3$, rt, 28 h, 95%; (d) compound 3, tert-butyl bromoacetate, NaI, Acetone, rt, 72 h, 37%. (e) K_2CO_3, DMF, 60°C, 72 h, 45%; (f) Trifluoroacetic acid/H_2O/Triisopropylsilane, rt, 2 h, 22%. (g) $TbCl_3 \cdot 6H_2O$, d.H_2O, pH ~5, rt, 17 h.

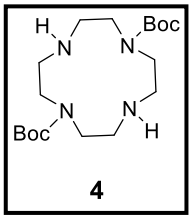

Cyclen (1.00 g, 5.80 mmol) was dissolved in $CHCl_3$ (0.06 M), to which Boc-OSu (2.50 g, 11.8 mmol) in $CHCl_3$ (0.24 mM) was added dropwise at room temperature. The solution was stirred for 28 hours at room temperature and washed with aq. NaOH (3M, 3 times). The organic layer was dried over K_2CO_3, filtered, and concentrated to yield 4 as a light brown powder (yield = 95%). ^{1}H NMR ($CDCl_3$, 500 MHz): δ 3.42 – 3.27 (8H, m), 2.91 – 2.73 (8H, m), 1.43 (18H, s). ^{13}C NMR (DMSO-d_6, 500 MHz): δ 155.3, 78.3, 49.3, 49.0, 28.1. LRMS (APCI$^+$): Calculated for $C_{18}H_{36}N_4O_4$, expected *m/z* 372.3, measured *m/z* 373.2 [MH^+].

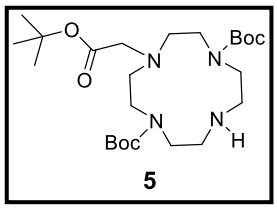

Compound **4** (1.77 g, 4.75 mmol) was dissolved in dry MeCN and stirred at 0°C under argon. Tert-butyl bromoacetate (0.70 mL, 4.8 mmol) was then added dropwise to the solution at 0°C under argon. The reaction was allowed to proceed for 48 hours, after which the reaction mixture was concentrated and dissolved in $CHCl_3$. Subsequently, it was washed with aq.NaOH (3M, 3 times), dried over K_2CO_3, filtered, and concentrated. The resulting oily residue was purified by flash chromatography (silica, CH_2Cl_2:$CHCl_3$:MeOH = 35:35:30 with 2% (v/v) NH_4OH), yielding **5** as an ivory solid (yield = 37%). ^{1}H NMR ($CDCl_3$, 500 MHz): δ 4.22-2.80 (18H, m), 1.45 (27H, m). ^{13}C NMR (DMSO-d_6, 500 MHz): δ 168.8, 154.96, 154.61, 81.3, 80.0, 49.5, 47.0, 46.5, 44.4, 27.8, 27.7. LRMS (APCI$^+$): Calculated for $C_{24}H_{46}N_4O_6$, expected *m/z* 486.3, measured *m/z* 487.3 [MH^+].

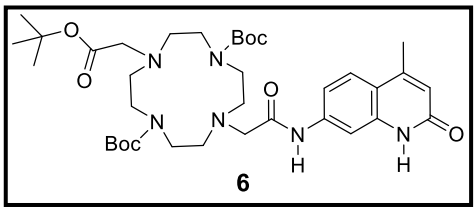

To compound **5** (0.200 g, 0.411 mmol) in DMF (0.041 M), bromo-acetyl Carbostyril-124 (**2**) (0.115 g, 0.389 mmol) and K_2CO_3 (80 mg, 0.59 mmol) were added. The reaction mixture was degassed and heated at 60°C under argon. After 72 hours, the reaction was cooled to room temperature and diluted with ethyl acetate, followed by washing with H_2O (3 times) and brine. The organic layer was dried over $MgSO_4$, filtered through a frit, and concentrated to result in a brown oil. This crude product was purified by flash chromatography (silica, $CHCl_3$:MeOH = 95:5), yielding **6** as a yellow oil. (yield = 45%) ^{1}H NMR($CDCl_3$, 500 MHz): δ 10.16 (1H, s), 9.48 (1H, s), 8.05 (1H, s), 7.56 (2H, m), 6.40 (1H, s), 3.52– 2.94 (20H, m), 2.44 (3H, s), 1.47 (27H, s). LRMS (APCI$^+$): Calculated for $C_{36}H_{56}N_6O_8$, expected *m/z* 700.4, measured *m/z* 701.3 [MH$^+$].

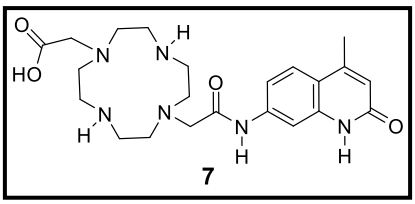

To Compound **6** (0.077 g, 0.11 mmol) dissolved in trifluoroacetic acid (5 mL) were added triisopropylsilane (0.125 mL) and d.H_2O (0.125 mL) at room temperature. The reaction mixture was stirred for 2 hours at room temperature and then concentrated under high vacuum, to which ether was added to precipitate out a crude product**.** This crude was dissolved in d.H_2O by adding NaOH to improve the solubility. The resulting solution was passed through a 0.45 μm filter and subjected to purification by RP-HPLC using a suitable linear gradient of MeCN containing 10% (v/v) de-ionized water (A) and H_2O containing 0.1% (v/v) TFA (B): 3-95% A over 30 min followed by returning to 3% A for equilibration. The fractions containing the product (retention time ~14.5 min) were collected, concentrated, and lyophilized to yield **7** as a white fluffy solid. (yield = 91%). ^{1}H NMR (DMSO-*d*$_6$, 500 MHz): δ 12.91 (1H, bs), 11.63 (1H, s), 10.49 (1H, s), 9.22 (1H, bs), 7.66 (1H, d, *J* = 8.5), 7.61 (1H, s), 7.47 (1H, d, *J* = 9.0), 7.28 (1H, bs), 6.29 (1H, s), 3.57 (2H, s), 3.52 (2H, s), 3.20 – 2.86 (16H, m), 2.38 (3H, s).^{13}C NMR (DMSO-*d*$_6$, 500 MHz): δ 170.7, 147.6, 140.1, 139.3, 125.6, 119.3, 118.2, 115.88, 115.80, 113.9, 104.9, 55.5, 53.5, 49.25, 48.8, 42.6, 42.5, 18.4. HRMS (HESI): Calculated for $C_{22}H_{32}N_6O_4$, expected *m/z* 444.25, measured *m/z* 445.33 [MH$^+$].

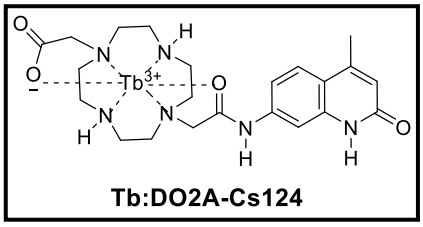

Compound **7** (20.6 mg) was dissolved in H_2O (40 mM) and treated with $TbCl_3 \cdot 6H_2O$ (1.0 equiv). The pH was adjusted to approximately 5 by slow dropwise addition of NaOH. The fluorescence of the solution was monitored over the next 5 days to confirm completion of the reaction. The resulting solution of **Tb:DO2A-Cs124** was obtained at a concentration of 20 mM.

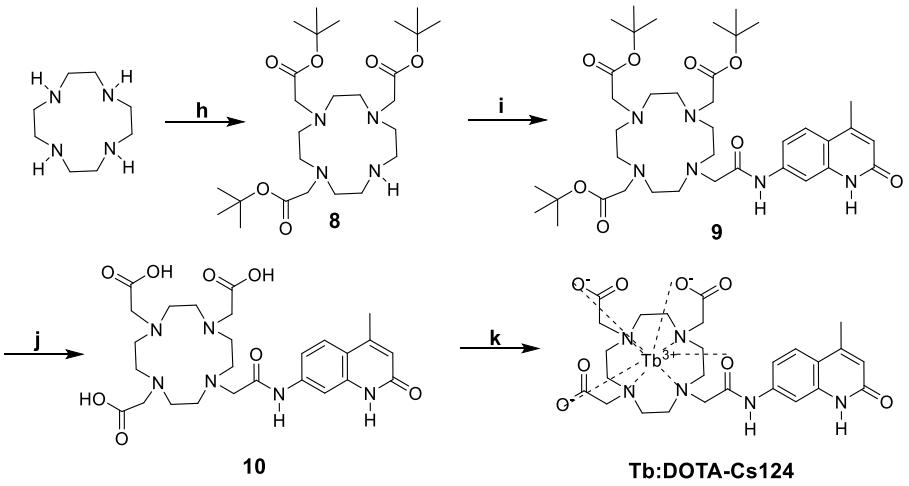

Scheme S3.

Conditions: (h) tert-butyl bromoacetate, $CHCl_3$, rt, 24 hours, 35%.(i) bromo-acetyl Carbostyril-124, K_2CO_3, DMF, 60°C, 72 hours, 45%; (j) Trifluoroacetic acid/H_2O/Triisopropylsilane, rt, 2 h, 22%. (k) $TbCl_3 \cdot 6H_2O$, d.H_2O, pH ~5, rt, 17 h.

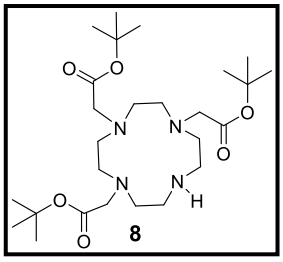

Cyclen (1.20 g, 6.97 mmol, 1 equiv.) was dissolved in dry MeCN and stirred at 0°C under argon. Tert-butyl bromoacetate (3.35 mL, 34.8 mmol, 5 equiv.) was then added dropwise to the solution. The ice bath was then removed, and the reaction proceeded at room temperature. After 72 hours, a white solid had formed and the reaction mixture was diluted in Ethyl Acetate, filtered and then concentrated. The solution was then recrystallized from toluene to yield **8** as a white solid (25% yield). ^{1}H NMR ($CDCl_3$, 300 MHz): δ 10.03 (1H, bs), δ 3.36 (4H,s), 3.28 (2H, s), 3.09 (4H, s), 2.91 (12H, m), and 1.45 (27H, s). ^{13}C NMR (DMSO-d_6, 500 MHz): δ170.6, 170.0, 128.9, 128.2, 80.5, 56.0, 52.1, 49.7, 48.4, 45.5, 30.7, 27.8. LRMS (APCI$^+$): Calculated for $C_{26}H_{50}N_4O_6$, expected *m/z* 514.4, measured *m/z* 515.2 [MH$^+$].

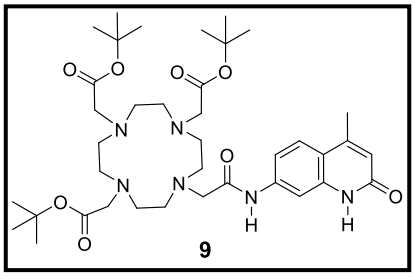

To compound **8** (0.2 g, 0.39 mmol, 1 equiv) in MeCN (20 mL), bromo-acetyl Carbostyril-124 (**2**) (0.11 g, 0.37 mmol, 1 equiv), and Cs_2CO_3 (0.19 g, 0.59 mmol, 1.5 eq) were added. The reaction mixture was degassed and heated at 60°C under argon. After 24 hours, the reaction was cooled to room temperature and diluted with ethyl acetate, followed by washing with H_2O (4x) and brine. The organic layer was dried over $MgSO_4$, filtered through a frit, and concentrated, giving compound **9** as a crude white solid which was utilized in the subsequent synthetic step without further purification.

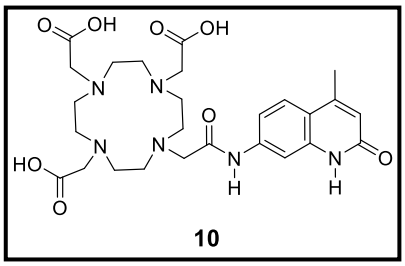

10

The t-butyl ester group of compound **9** (0.229 g) was converted to the corresponding acid by treating it with trifluoroacetic acid (9 mL) containing 2.5% v/v triisopropylsilane (TIPS) and 2.5% v/v H_2O at room temperature for 2 hours. The reaction mixture was then concentrated under high vacuum, and ether was added to precipitate the crude product **10.** The product was extracted using H_2O, and NaOH was used to enhance solubility. The resulting solution was filtered and subjected to purification by RP-HPLC using a suitable linear gradient of MeCN containing 10% (v/v) de-ionized water (A) and 0.1% (v/v) TFA/H_2O (B) (3-100% A over 30 min, followed by a sharp gradient to 97% B and returning to 80% A for equilibration). The fractions containing the product (retention time ~14.5 min) were collected and concentrated, yielding **10** as a white solid with a 71% yield after two steps. ^{1}H NMR (DMSO-*d*$_6$, 500 MHz): δ 11.50 (1H, s), 10.54 (1H, s), 7.64 (1H, d, J= 9Hz), 7.44 (1H, s), 7.21 (1H, d, J= 6.05Hz), 6.29 (1H, s), 3.74 (8H, s), 3.37-3.15 (16H, m), 2.38 (3H, d, J= 0.75 Hz). ^{13}C NMR (DMSO-*d*$_6$, 500 MHz): δ 171.1, 147.6, 140.1, 139.3, 125.5, 119.3, 118.4, 116.1, 115.9, 113.7, 104.6, 57.7, 55.6, 53.9, 53.5, 50.2, 50.0, 49.7, 49.5, 18.4. HRMS (HESI): Calculated for $C_{26}H_{36}N_6O_8$, expected *m/z* 560.26, measured *m/z* 561.42 [MH^+]. (We need 20)

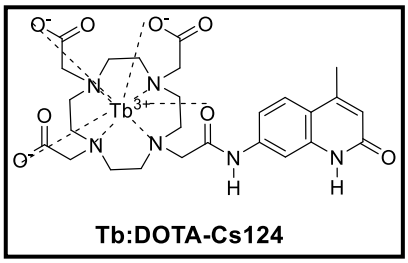

Tb:DOTA-Cs124

Compound **10** (21.6 mg) was dissolved in H_2O (40 mM) and treated with $TbCl_3 \cdot 6H_2O$ (1.0 equiv.). The pH was adjusted to approximately 5 by slow dropwise addition of NaOH. The fluorescence of the solution was monitored over the subsequent 5 days to confirm completion of the reaction. The resulting solution of **Tb:DOTA-Cs124T** was obtained at a concentration of 20 mM.

Part II: Photophysical Measurements

Added Anion	t_{H_2O} (ms)	t_{D_2O} (ms)	*q*
None	0.98	2.02	2.36
+ Citrate	1.31	1.45	0.06
+ Phosphate	1.34	1.75	0.59
+ PPi	1.37	1.79	0.56
+ Bicarbonate	1.21	2.05	1.39
+ Malonate	1.68	1.94	1.07
+ Isocitrate	1.39	1.67	0.30

Table S1: Water Cooridantion Number (q) of Tb:DO2A-Cs124 in the presecen of various anions determined from change in luminescent lifetimes in H_2O and D_2O

Added Anion	t_{H_2O} (ms)	t_{D_2O} (ms)	*q*
None	1.59	2.50	0.85

Table S2: Water Cooridantion Number (q) of Tb:DOTA-Cs124 in the presecen of various anion determined from change in luminescent lifetimes in H_2O and D_2O

Part III: Luminescence Spectra

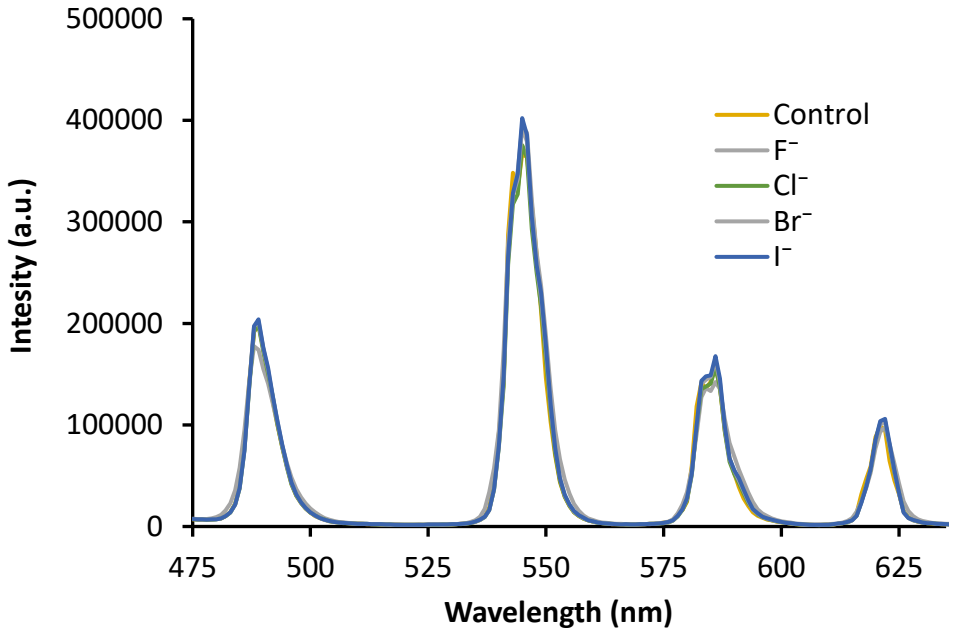

Figure S1. a) Emission of Tb:DO2A-Cs124 in the presence of various halides. Experimental condition: [Tb:DOTA-Cs124] = 10 mM in H_2O, pH 7, [anion] = 1 mM, l_{ex} = 340 nm. Intensity is the normalized sum of emission intensities from 530 – 560 nm based on the control in the absence of anions.

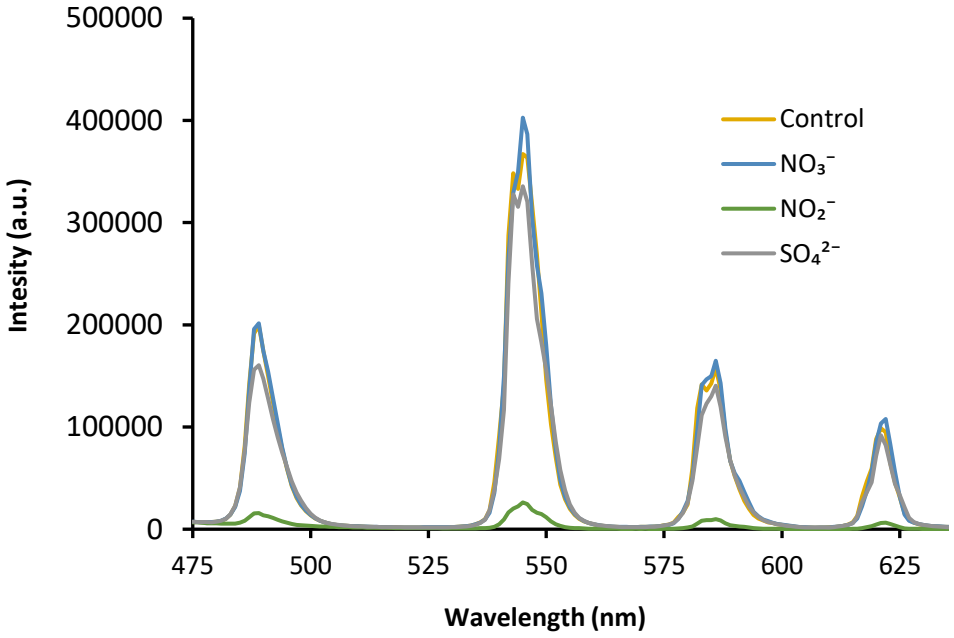

Figure S2. a) Emission of Tb:DO2A-Cs124 in the presence of various Oxoanions. Experimental condition: [Tb:DOTA-Cs124] = 10 mM in H_2O, pH 7, [anion] = 1 mM, l_{ex} = 340 nm. Intensity is the normalized sum of emission intensities from 530 – 560 nm based on the control in the absence of anions.

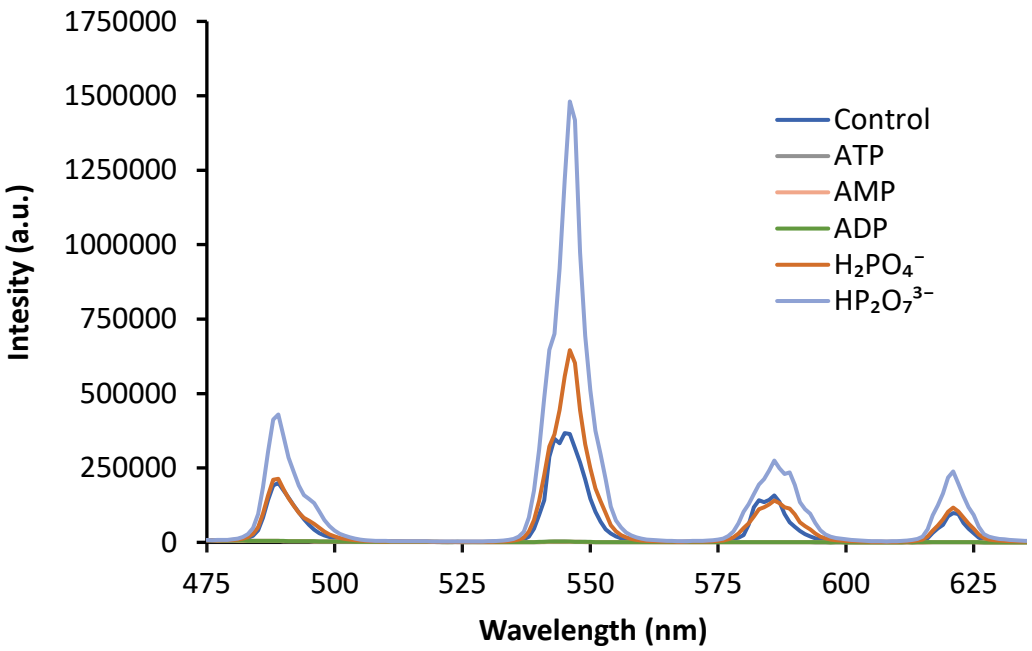

Figure S3. a) Emission of Tb:DO2A-Cs124 in the presence of various phosphate containing anions. Experimental condition: [Tb:DOTA-Cs124] = 10 mM in H_2O, pH 7, [anion] = 1 mM, l_{ex} = 340 nm. Intensity is the normalized sum of emission intensities from 530 – 560 nm based on the control in the absence of anions.

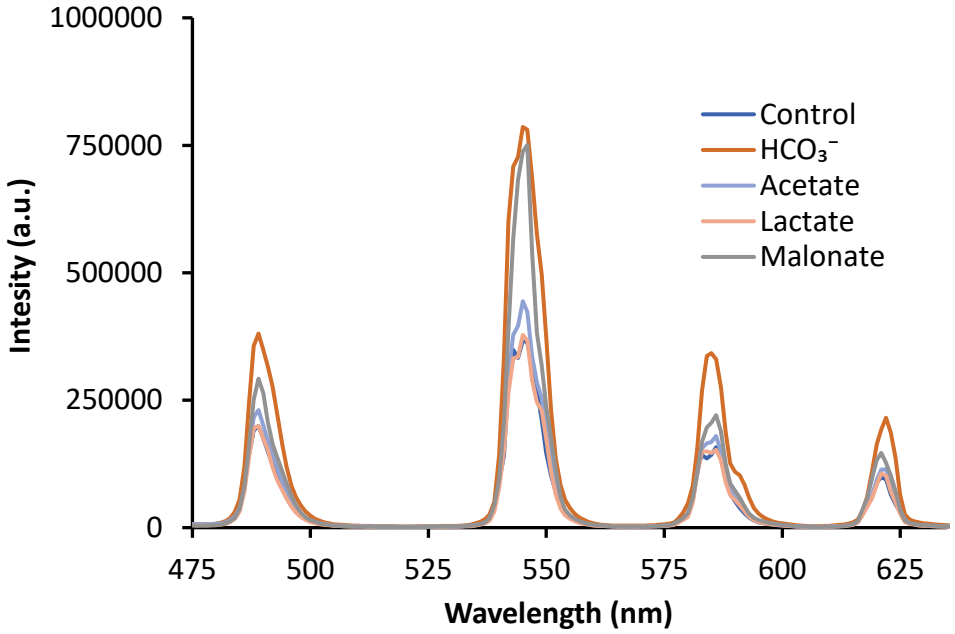

Figure S4. a) Emission of Tb:DO2A-Cs124 in the presence of various metabolic carboxylates. Experimental condition: [Tb:DOTA-Cs124] = 10 mM in H_2O, pH 7, [anion] = 1 mM, l_{ex} = 340 nm. Intensity is the normalized sum of emission intensities from 530 – 560 nm based on the control in the absence of anions.

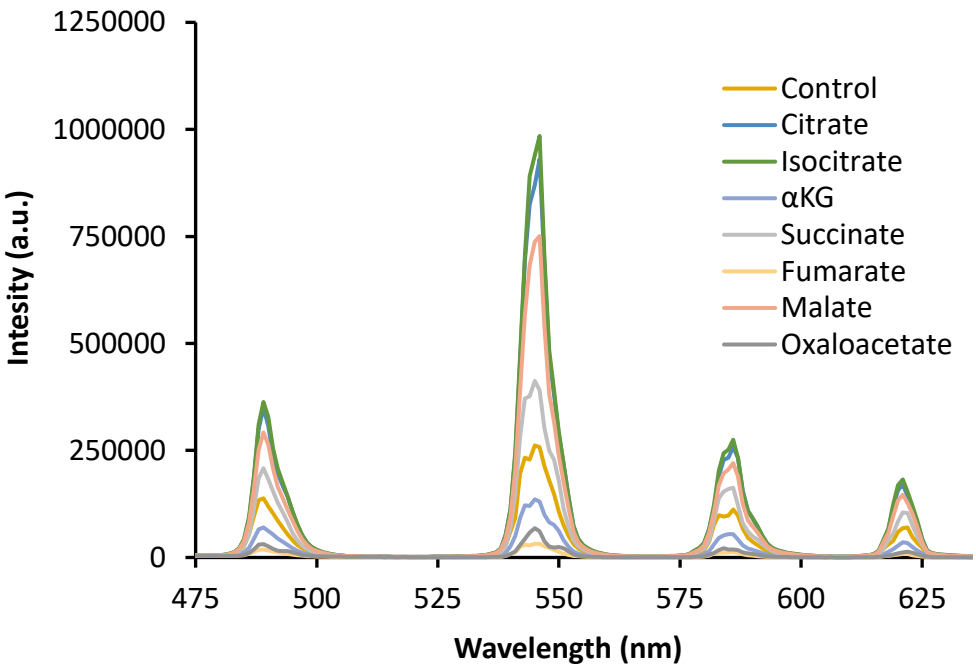

Figure S5. a) Emission of Tb:DO2A-Cs124 in the presence of various Citric Acid Cycle (CAC) intermediates. Experimental condition: [Tb:DOTA-Cs124] = 10 mM in H_2O, pH 7, [anion] = 1 mM, l_{ex} = 340 nm. Intensity is the normalized sum of emission intensities from 530 – 560 nm based on the control in the absence of anions.

Part IV: ^{1}H and ^{13}C NMR Spectra

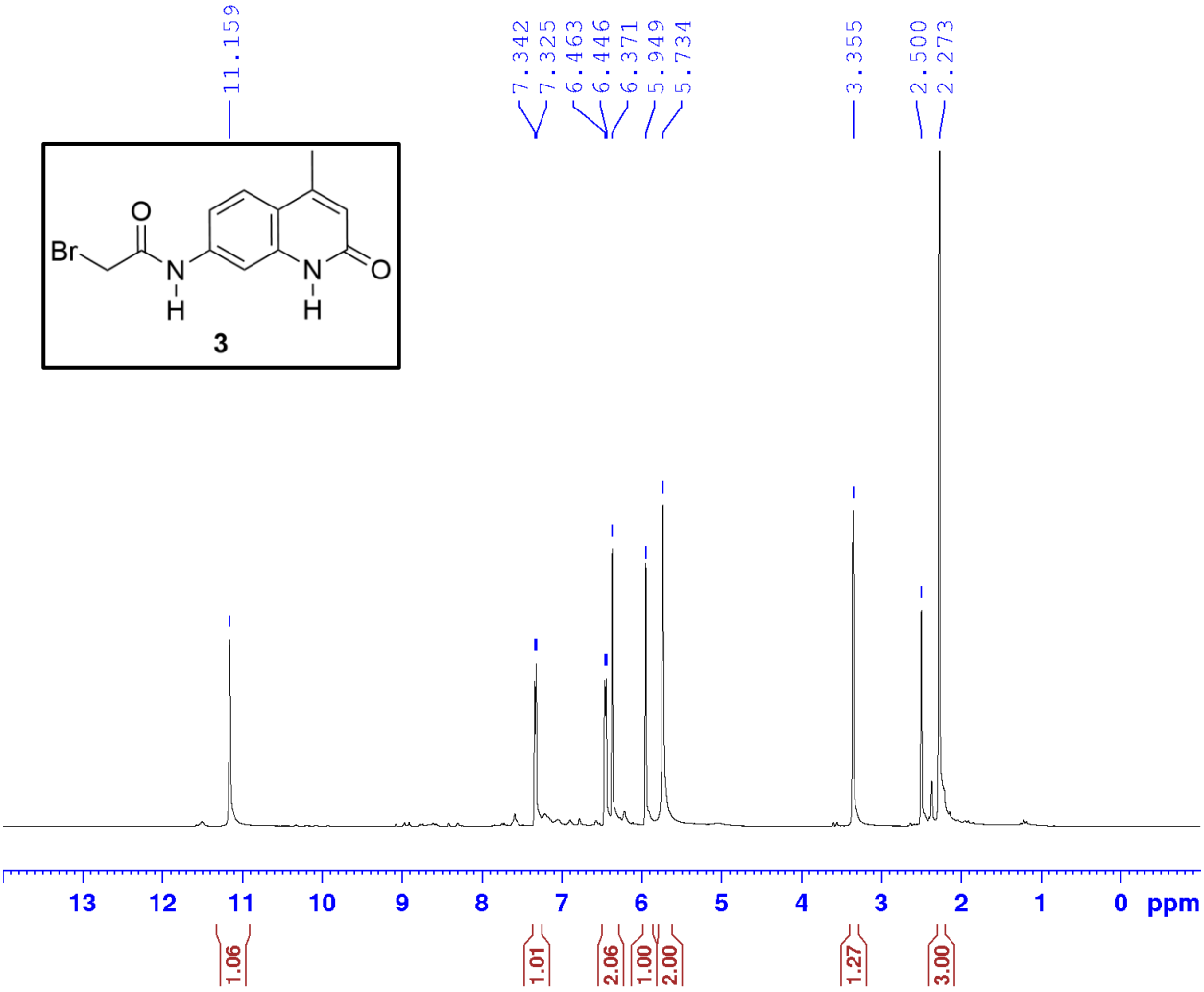

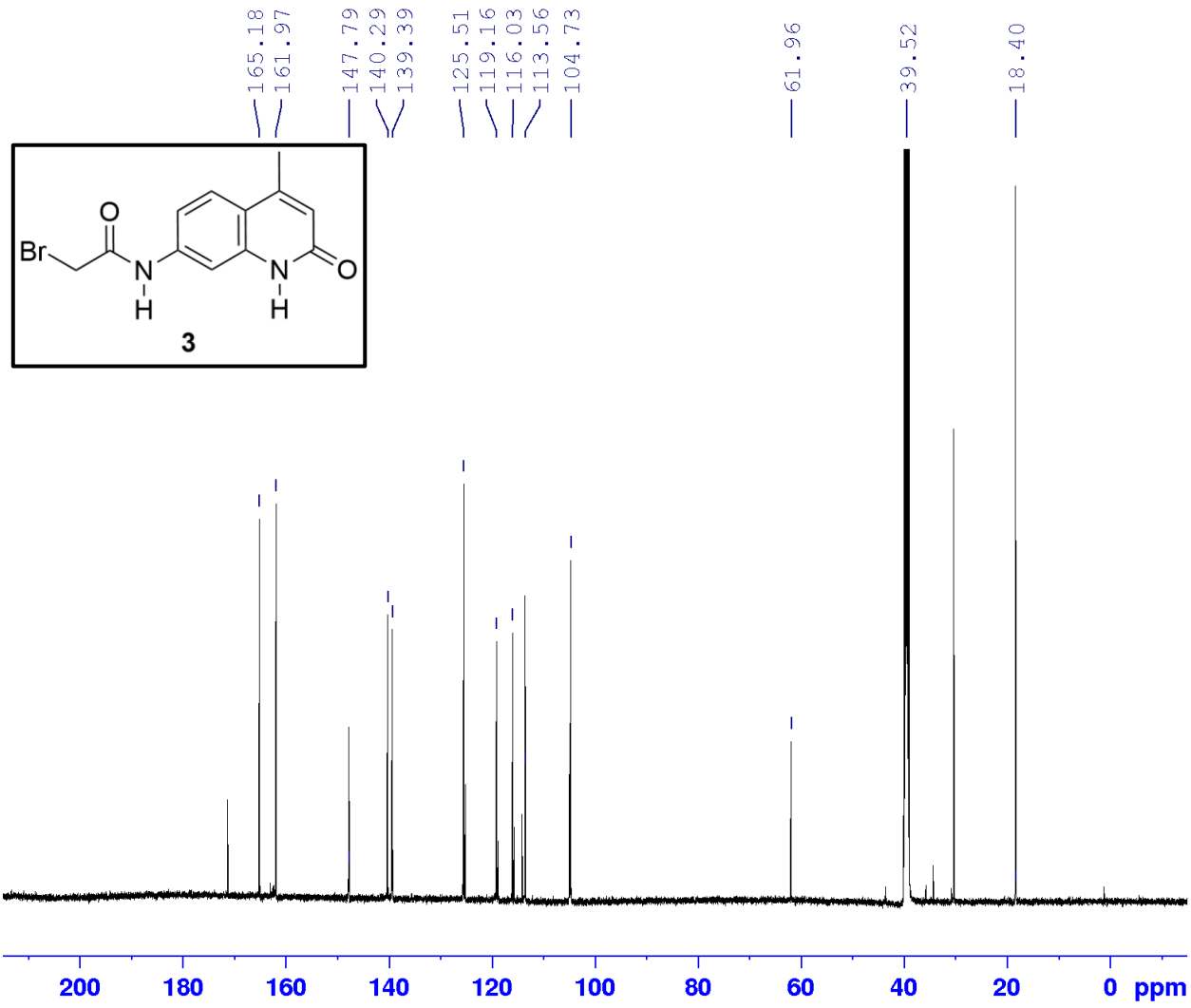
165.18
161.97
147.79
140.29
139.39
125.51
119.16
116.03
113.56
104.73
61.96
39.52
18.40
Br
O
N
H
O
N
H
O
3
200
180
160
140
120
100
80
60
40
20
0
ppm

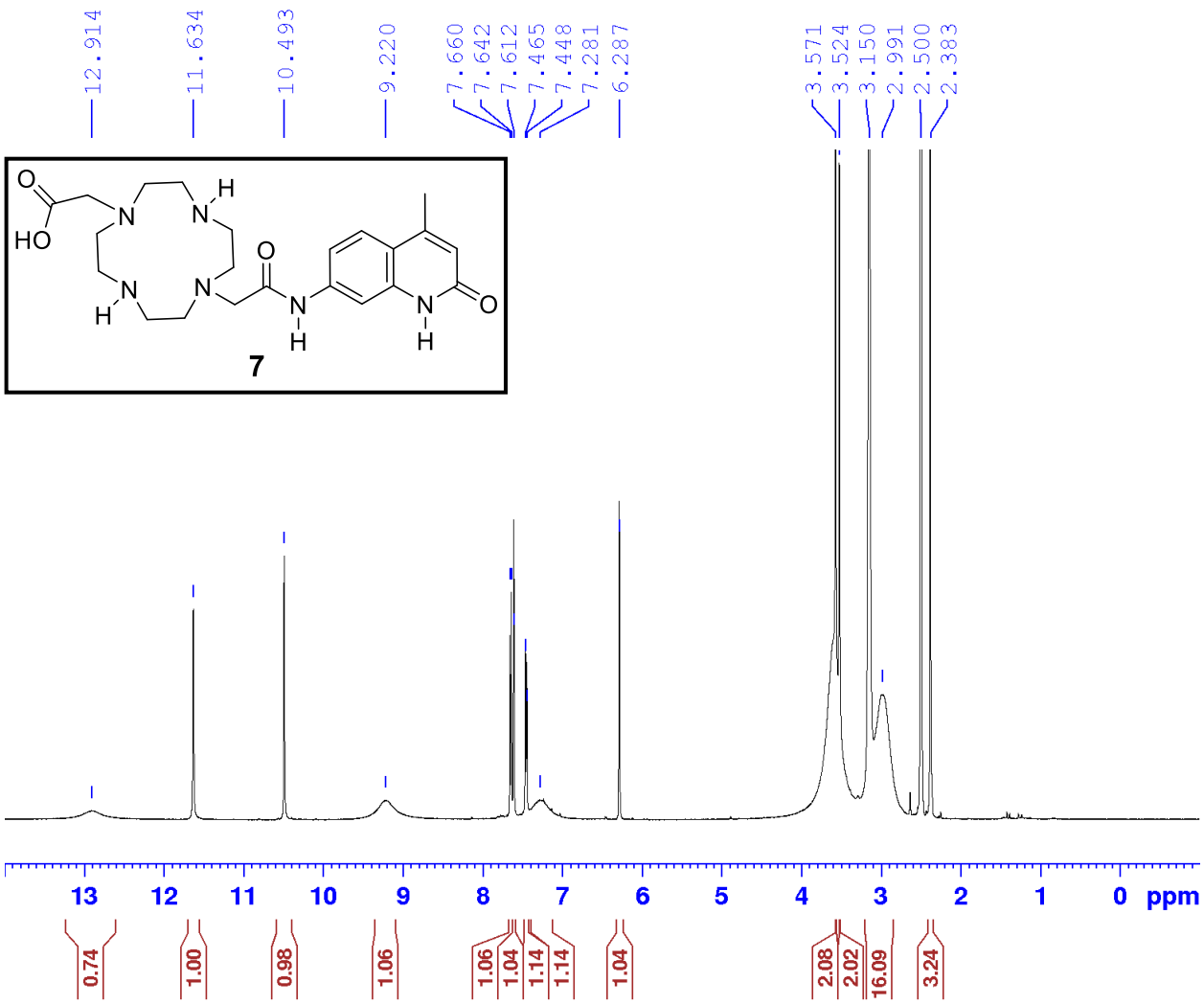
12.914
11.634
10.493
9.220
7.660
7.642
7.612
7.465
7.448
7.281
6.287
3.571
3.524
3.150
2.991
2.500
2.383
7
13
12
11
10
9
8
7
6
5
4
3
2
1
0
ppm
0.74
1.00
0.98
1.06
1.06
1.04
1.14
1.14
1.04
2.08
2.02
16.09
3.24

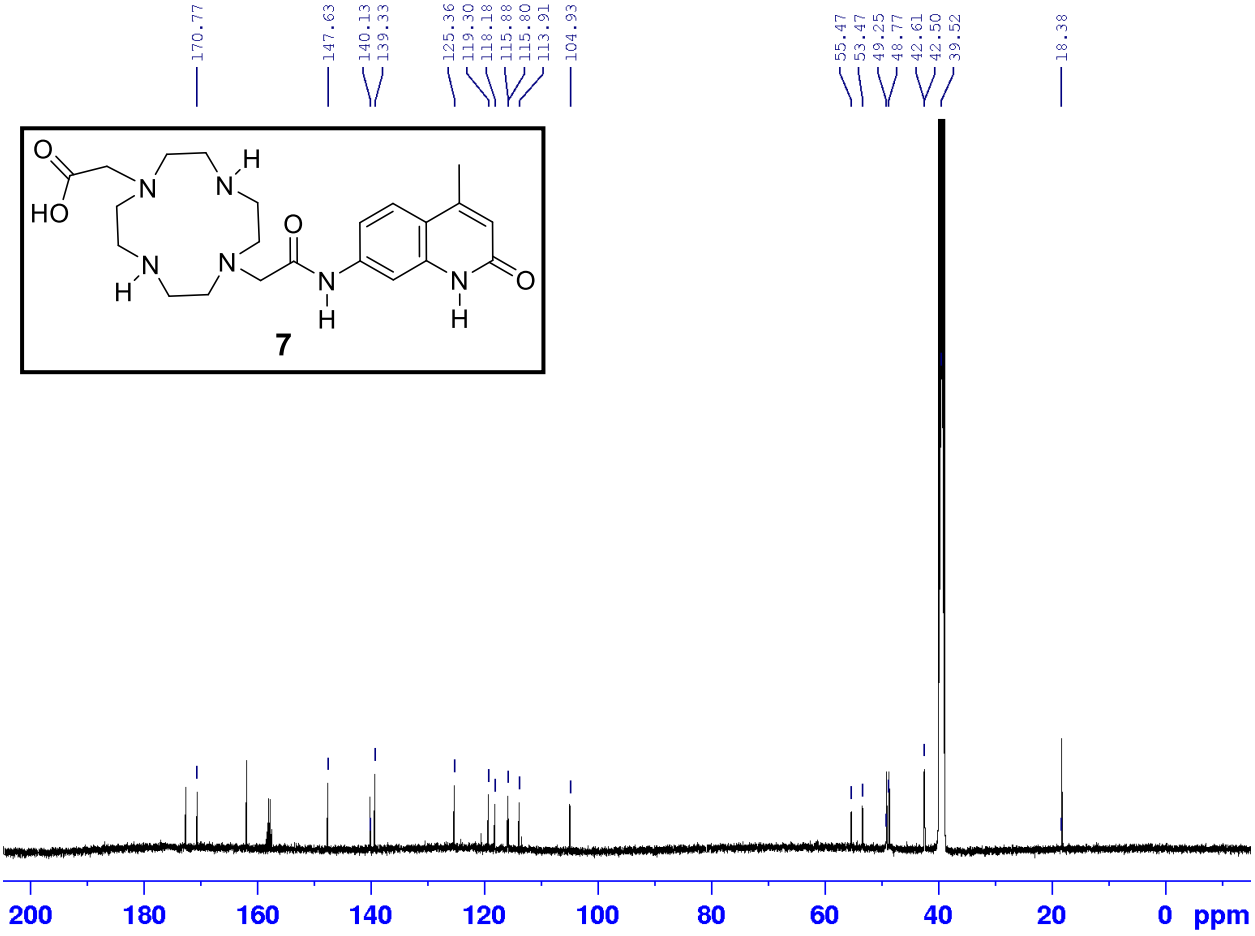
170.77
147.63
140.13
139.33
125.36
119.30
118.18
115.88
115.80
113.91
104.93
55.47
53.47
49.25
48.77
42.61
42.50
39.52
18.38
7
200
180
160
140
120
100
80
60
40
20
0
ppm

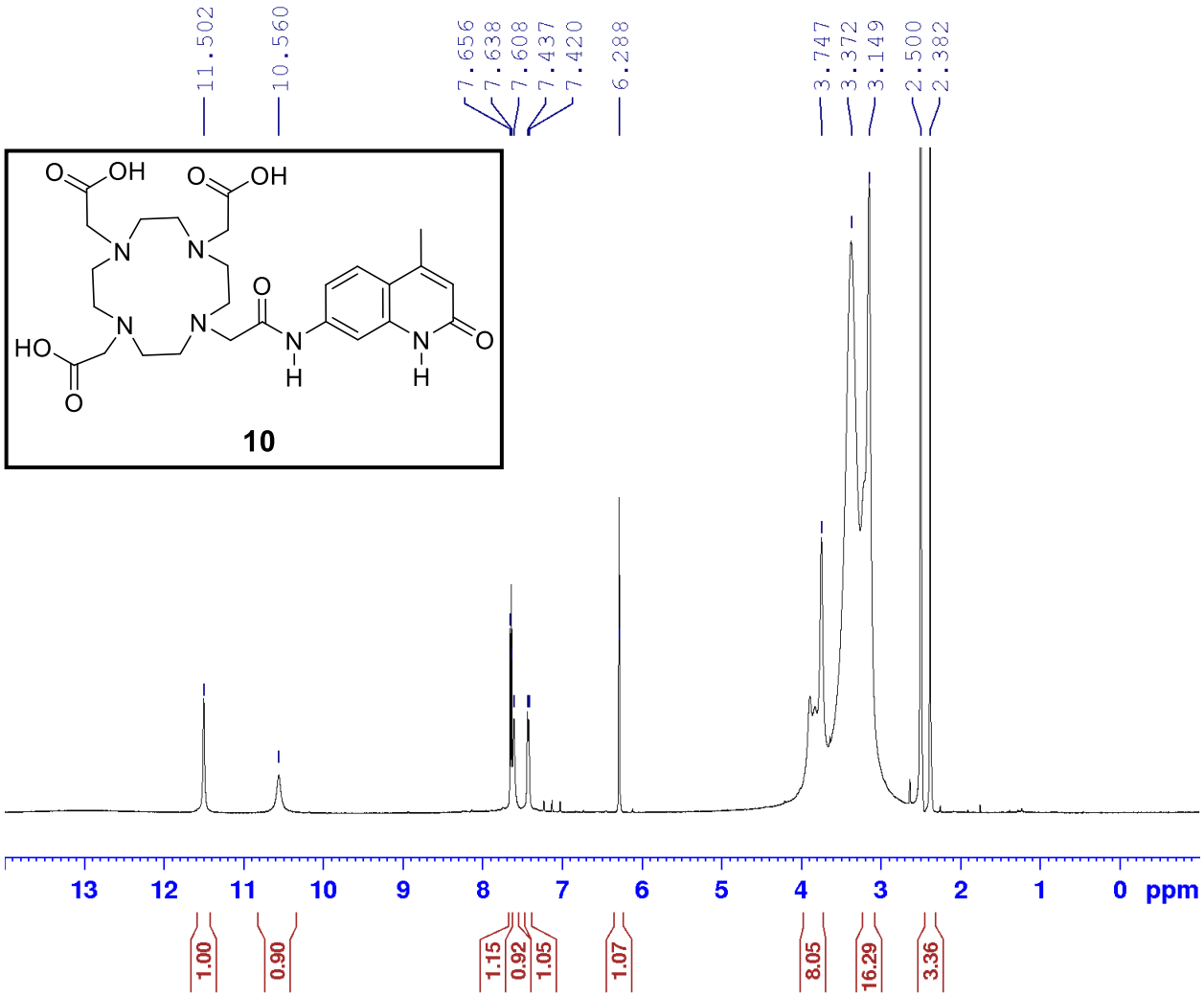
11.502
10.560
7.656
7.638
7.608
7.437
7.420
6.288
3.747
3.372
3.149
2.500
2.382
10
13 12 11 10 9 8 7 6 5 4 3 2 1 0 ppm
1.00
0.90
1.15
0.92
1.05
1.07
8.05
16.29
3.36

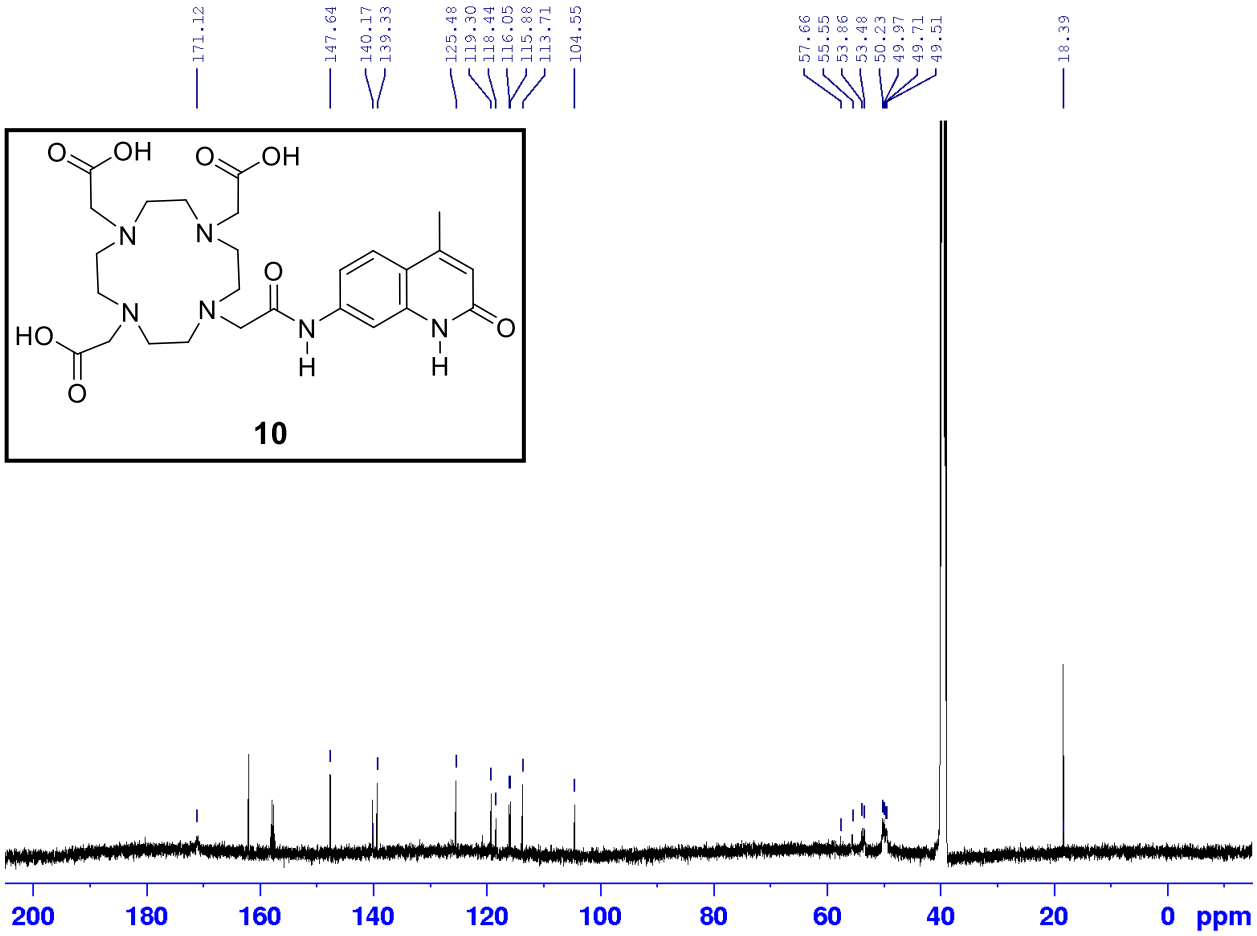
171.12
147.64
140.17
139.33
125.48
119.30
118.44
116.05
115.88
113.71
104.55
57.66
55.55
53.86
53.48
50.23
49.97
49.71
49.51
18.39
10
200
180
160
140
120
100
80
60
40
20
0
ppm

Appendix

Honors Symposium Speech

Panel title: Pathways to Innovation: Unveiling Science's Journey from Inquiry to Truth

Presented May 18, 2024

A crucial tool needed in biological and environmental research is the ability to detect and visualize the presence of a particular target of interest. Take for example cellular biology, where understanding both where and when cellular processes are occurring are key to further uncovering the intricacies of the field. Or, for example, conservation biology, where understanding the concentrations of harmful toxins in water is extremely relevant. All these fields of research are driven by instruments that allows for the detection of such cellular events, or such water toxins. Consequently, improving the detection of targets of interest has become a key focus in developing more sensitive, accurate, and reliable tools for addressing research questions. Over the years, complex machines have been made to detect many different types of samples. Examples of this include using mass spectrometry, which is able to detect different chemicals present in a sample. Additionally, there are different types of machines that are able to detect fluorescent and luminescent signals of samples. This detection technique is especially relevant in biological sciences and was the focus of my research.

To better understand the focus of my research, I will first walk you through an example of fluorescent tagging. Imagine you have a massive textbook with thousands of words, and you want to find all the important terms quickly. Instead of reading every single word, you use a highlighter to mark the key terms. When you flip through the pages later, the highlighted terms stand out, making them easy to spot.

In immunology, scientists need to find and study specific cells or proteins within a complex biological sample. They use organic fluorophores, which act like the highlighter. These fluorophores are special molecules that glow when exposed to certain light. Scientists attach these glowing markers like the red dot, to antibodies, the Y shaped structure, that can then attach to the cells or proteins they are interested in. When they shine a special light on the sample, the fluorophore glows red, highlighting the precise location of the target cells or proteins. This glowing effect makes it much easier for scientists to identify and study these important biological components, just like how highlighted text stands out in a book.

Significant research efforts are being dedicated to advancing imaging technologies. The goal is to make these systems cheaper, more accessible, and applicable to a broader range of questions. In recent decades, there has been a growing interest in using lanthanide metals as luminescent sensors to highlight molecules rather than using the red fluorophore from the figure. These lanthanide sensors usually contain the elements terbium or europium, and possess unique properties that set them apart from previously used fluorophores. These properties include sharp emission bands like seen on the right, and long luminescent lifetimes, both of which can prove useful when tagging molecules in complicated environments with high sensitivity.

The research I worked on involved developing two special terbium complexes to study how different chemical environments affect their properties. Imagine we created two different "chemical probes" to see how they behave. Each of these probes has three main parts: A lanthanide metal core. A ring-like structure that holds the metal. And an antenna that attaches to the ring. The antenna helps absorb UV light and transfer the energy to the metal, resulting in the lighting up of the probe.

The different feature of these probes is the number of connections the terbium metal has. Terbium can connect to nine different spots, but in our designs, not all spots are filled:

Here are the luminescent compounds that were made. The one on the top is called DO-2-A and has six connections to the Terbium metal indicated by the dashed lines. The different parts that connect to the green Terbium are the ring structure seen in brow and the energy transferring antenna seen in blue. This design leaves three spots of the metal unoccupied. The second compound that was made is called DO-T-A and had eight connections. This probe also has a ring-like structure, shown here in pink, along with the same blue antenna. You'll notice that the ring structure looks a bit different in this probe because it has more branch-like structures which change the number of open spots in the probes. The reason we left some spots unconnected is because water molecules can fill those spots. When water attaches to the metal, it reduces its ability to glow as seen on the left. So, in water, the first probe would have three water molecules attached, and the second probe would have one, affecting how they glow.

This design of leaving some spots open is what allows us to use these probes to highlight negatively charged molecules called anions. When these negatively charged anions are in the same liquid as the probes, they interact with a part of the probe that has a positive charge. This interaction

is stronger than the one between the probe and the water molecules around it. So, the anions push away the water molecules and make the probe glow as see on the right. This design is thus a switch light mechanism: when the chemical probe is water, it's turned off, but as soon as an anion is present, the probe will light up for us to see.

The main difference between these probes is their overall charge, where the D-O-2-A has a +2 net charge and the D-O-T-A probe has a net zero charge. This leads them to have different attractions to the negative anions and thus detect different molecules.

To make these probes, you can imagine it like making a big Lego piece. Instead of making it all in one go, we decided to break it up into smaller parts. Making the antenna first, purifying it, and making sure to add a connecting piece to one end so that it could be attached to the ring. Next, we made the two different rings with their corresponding branches coming off of them. The rings had the same base, and then it was just a matter of attaching the right number of branches. This too was followed by purification steps to ensure that we could use the compounds in following reactions. The final step was then combing all the pieces together as demonstrated to make the two probes. All these steps are important to ensure that the synthesis had the highest chance of making our desired probes. The Lego-building analogy can further be taken to this research process by highlighting that, oftentimes, when trying to generate novel compounds like one ones that we made, the protocols aren't in place. In a similar fashion, this would be like not having the manual for the given Lego set you're trying to make. But like trying to make Legos without instructions, breaking down the process into small, manageable steps, helps you create the bigger piece.

In research, we often do this by looking at past studies to find similarities, even if they're not exactly the same as what we're doing. These similarities can give us clues on how to create the smaller parts needed for our own work. To do this, we build on what we already know about chemical reactions and lanthanide probes. But it's not just about planning; this process also involves a lot of trial and error. Despite reading many published works to find the best approach, it's impossible to predict exactly how everything will come together until we try it ourselves. This highlights the dynamic and iterative nature of science, where experimentation and learning from mistakes are essential, even though they're sometimes overlooked during presentations and publications.

Ultimately, once we had created our probes, we set out to test them in the presence of different anions. We screened each probe individually with 20 different anions that include a wide range of biochemically and environmentally relevant anions to see what our probes could detect. Here are the results of the screening. Below the D-O-T-A probe on the left is the relative light intensity of D-O-T-A in the presence of anions. These results indicate that in presence of the different anions, D-O-T-A did not seem to have drastic changes in glow, indicating that it was not turned on by any of the anions. We can come to understand this from potentially the probes' 3-d geometry resulting from the branch groups wrapping around the metal core, forming a basket like structure that might prevent the water from being pushed out, making it more resistant to change. This structure also has a net charge of zero, meaning that negative anions aren't as attracted and are less like to push out the water. Surprisingly, the only drastic change was from the anion Nitrite. When investigating the results, the answer as to why nitrite decreased the base glow of the probe wasn't clear, but upon better understanding how the energy from the antenna was being transferred, we came to understand that Nitrite, the negative anion, was most likely absorbing the energy from the antenna before it reached the Terbium. This in turn decreased the energy going to the "light bulb" of the probe, decreasing its glow.

The D-O-2-A probe, on the other hand, had a much more exposed terbium core and it had a net charge of +2, which, in theory, would make anions more strongly attracted to the metal, and thus more likely to dispel the water molecules. This is in fact what was observed. The D-O-2-A probe had much more pronounced changes upon the addition of anions. The most drastic changes observed were specific to a class of anions called carboxylates. Notably, this class of anions include many metabolically relevant anions, including acetate, malonate, citrate, and lactate. The probe has a particularly large emission increase of 3 fold by citrate, and we expected this to be a result of the displacement of all three water molecules. A proposed model for this interaction is as follows, where the addition of the citrate results in the waters being kicked off the metal and new connections being formed with the citrate production.

Due to D-O-T-A being a highly selective detector of nitrite amongst a diverse range of anions, a promising application for this probe in detecting nitrite within complex cellular or environmental media that have many anions present. An example of this application is using this

probe to test water samples to identify potential nitrite contamination in farm water where nitrite rich-fertilizer is used.

For D-O-2-A, while it might not work well within complex cellular media due to it's wide reactivity, our findings highlight the potential utility of D-O-2-A to study the speed of enzymes like citrate synthase by monitoring the change in glow over time as citrate is produced. Additionally, it could also help testing substances that block or compete with the enzyme by again monitoring changes in glow that result from the citrate.

This research underscores the dynamic nature of science. The journey began by identifying a gap in imaging technologies and leveraging past discoveries and knowledge to drive innovative inquiries. While we started with a solid foundation, generating novel solutions required more than just applying previous knowledge—it required synthesizing it in new ways.

In our case, this meant combining established understanding of lanthanide metals with theoretical knowledge of chemical reactions to create new molecules that address existing gaps. This approach not only advanced our research but also highlighted the iterative and evolving process of scientific discovery. By building on what was known and creatively applying it, we were able to develop innovative probes with promising applications in detecting nitrite and studying enzyme activity. This synthesis of past and present knowledge exemplifies how science continually evolves to solve new challenges. Ultimately embodying the creation of knowledge.